

# High Selectivity SIW Cavity Bandpass Filter Loaded CSRR with Perturbing Vias for Sub-6 GHz Applications

N. Praveena\* and N. Gunavathi

**Abstract**—A narrowband, high selectivity Substrate Integrated Waveguide (SIW) bandpass filter with perturbing vias and CSRR is proposed for Sub-6 GHz applications. Firstly, the perturbing vias are positioned at the symmetrical axis of the SIW cavity which produces distinct electric field distribution for the first two modes. Next, the ground plane is engraved with the CSRR placed at an offset distance on either side of the perturbing vias, forming the coupling arrangement that combines mixed and magnetic, electric coupling. The presence of CSRRs resulted in a narrowband filter. The filter's center frequency is 4.947 GHz with a fractional bandwidth of 1.16%. By comparing the fabricated filter to an existing SIW conventional multi-cavity or cascaded resonator, a size reduction of 117% is achieved. The simulated and measured results agree with each other.

## 1. INTRODUCTION

Amid the fast growth of present wireless communication systems, compact size, low loss, and highly integrable microwave bandpass filters are immediately required. The Chinese government approved the sub-6 GHz frequency bands, such as 3.3 to 3.6 GHz and 4.8 to 5 GHz, for 5G applications [1]. The planar technology resonators such as microstrip and coplanar waveguide (CPW) has lower unloaded quality factor (QUL) and not appropriate for filters of narrowband with fractional bandwidth less than 2% for frequency above 1 GHz [2, 3]. Hence, the new transmission line SIW emerges to overcome the drawbacks of conventional rectangular waveguide's high cost, large size, difficulty in planar integrations and planar structures (microstrip, CPW) radiation loss, and packaging problems [4]. However, to attain high selectivity, the cascading of multiple cavities leads to a larger size filter. Therefore, compact size and more number of transmission zeros are trade-off criteria in designing a high selectivity filter. The multimode/dual mode SIW filters are extensively used to reduce the number of cavities and maintain better response [5–7, 10]. The frequently used SIW filters are of a dual-mode square cavity, created by placing extra metallic via holes acting as perturbations ( $TE_{201}$  and  $TE_{102}$ ). Though the structures loaded with coplanar strip, complementary split ring resonator, and coplanar waveguides on the upper metal layer of the SIW filter form the multi-mode filters reported in [8, 10, 11], the above hybrid structures lead to larger radiation loss due to the breakdown of shielding and integrity of the SIW cavity [12, 13].

This article presents a SIW cavity bandpass filter loaded with complementary split-ring resonator (CSRR) on either side of perturbing vias. The  $Q$  factor of the proposed filter is 302. The narrowband SIW filter of second order with two transmission zeros is proposed for sub-6 GHz applications. By comparing the fabricated filter to a conventional multi-cavity or cascaded resonator, a size reduction of 117% is achieved.

---

Received 20 December 2022, Accepted 10 March 2023, Scheduled 18 March 2023

\* Corresponding author: Namanathan Praveena (praveenanittece@gmail.com).

The authors are with the Department of Electronics and Communication Engineering, National Institute of Technology Tiruchirappalli, India.

## 2. DESIGN ANALYSIS

### 2.1. SIW Geometry

The designed SIW filter comprises CSRRs and perturbing vias used for sub-6 GHz wireless applications. Firstly, the filter is designed with perturbing vias placed on the symmetrical axis on the center of the cavity. Next, the CSRRs are loaded with a offset distance of  $e_1$ ,  $e_2$  on either side of the perturbing vias.

Figures 1(a) and (b) depict the front view and back view of the proposed filter. The SIW square cavity with a metallic hole of diameter ' $d$ ' is separated with a pitch distance ' $s$ ' which should follow the rules  $\frac{d}{\lambda_0} \leq 0.1$  and  $\frac{d}{p} \geq 0.5$  to avoid metallic via leakage ( $\lambda_0$  represents the free-space wavelength).

$W_{ef} = W_s - \frac{d^2}{0.95 \times p}$ ,  $L_{ef} = L_s - \frac{d^2}{0.95 \times p}$ . Here  $W_s$  and  $L_s$  are width and length of the SIW.

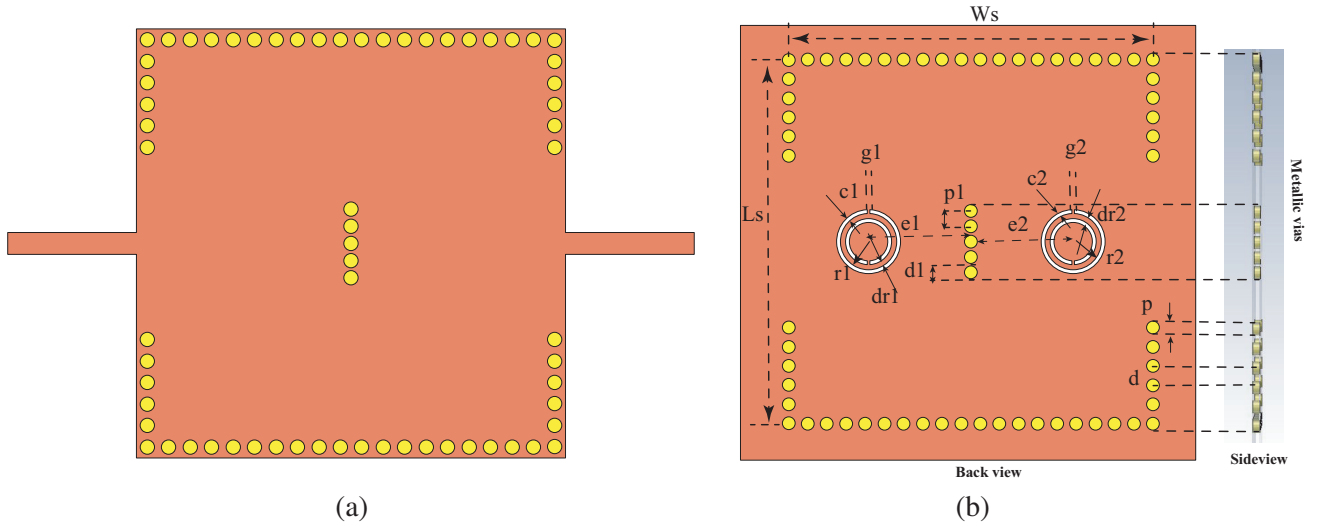


**Figure 1.** Proposed filter. (a) Front view. (b) Back view. The variable values are  $W_s = 28.4$ ,  $L_s = 28.4$  mm,  $p = 1.5$  mm,  $d = 1$  mm,  $p_1 = 1.2$  mm,  $d_1 = 1$  mm,  $d_{r1}$ ,  $d_{r2} = 0.4$  mm,  $r_1$ ,  $r_2 = 2.5$  mm,  $c_1$ ,  $c_2 = 0.3$  mm,  $g_1$ ,  $g_2 = 0.2$  mm,  $e_1$ ,  $e_2 = 8$  mm.

The resonant frequency ( $f_{mn0}$ ) of SIW cavity for  $TE_{mn0}$  is given by [9]

$$f_{mn0} = \frac{c}{2 \times \sqrt{\epsilon_r}} \sqrt{\left(\frac{m}{W_{ef}}\right)^2 + \left(\frac{n}{L_{ef}}\right)^2} \quad (1)$$

Here  $W_{ef}$  and  $L_{ef}$  are the effective width and effective length of the SIW.

The simulated eigen-mode field distributions of the two modes (mode1, mode2) using Computer Simulation Technology (CST) is depicted in Figures 2(a) and 2(b). The perturbing vias at the center symmetrical axis of the cavity produce two perturbed modes which are different from the cavity without perturbing vias. The unloaded cavity field distribution differs from that of the perturbed modes. Hence, two modes are closer in the proposed filter, and a high unloaded quality factor, two-pole, narrowband filter is designed using single cavity without occupying extra area. The two perturbed modes created are coupled using CSRR, and CSRR provides positive coupling with two transmission zeros. The CSRR is an electric dipole in nature and is excited axially by an electric field which offers narrow bandwidth for the proposed filter. The coexistence of electric and magnetic coupling due to perturbing elements and the CSRR provides mixed-coupling in the proposed structure.

### 2.2. Equivalent Circuit and Field Distribution

The LC circuit for the proposed narrowband filter is shown in Figure 2(c). The CSRR's  $R_1$  and  $R_2$  are denoted by  $L_a$  and  $C_a$  in the equivalent circuit. The metallic vias, which act as a side wall for

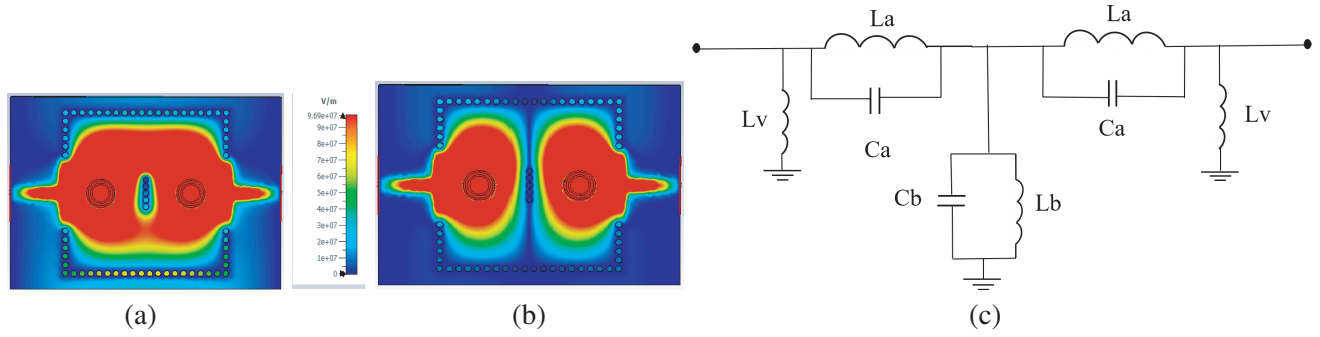


Figure 2. E field distribution. (a) mode1. (b) mode2. (c) LC circuit.

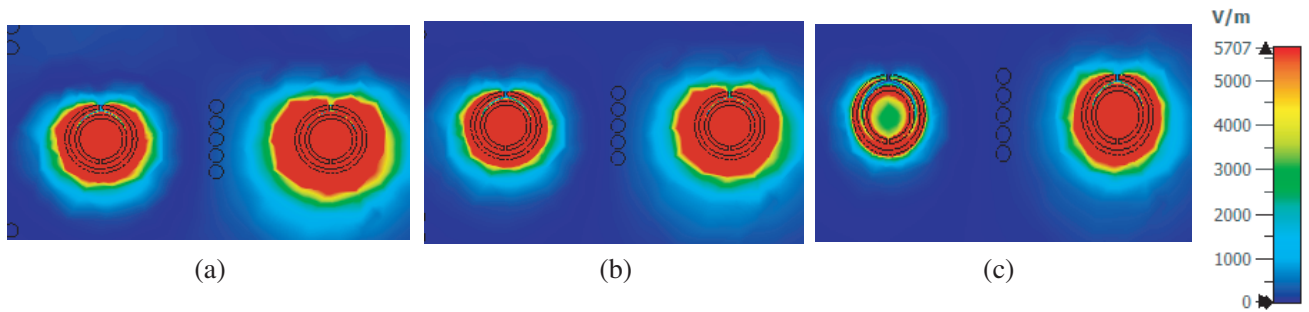


Figure 3. Field distribution at (a) 4.8 GHz, (b) 4.96 GHz, (c) 5 GHz.

the SIW cavity, are indicated as shunt inductor  $L_v$ . The perturbing element at the middle of the SIW cavity is denoted as  $L_b$  and  $C_b$  of the tank circuit. The circuit configuration implies that the mixed coupling geometry exists in the proposed filter. The perturbing vias and CSRRs are placed at an offset distance with a slit gap oriented towards the top forming the mixed coupling geometry. The electric field distribution at lower out-of-band is 4.8 GHz; center frequency is 4.96 GHz; and upper out-of-band is 5 GHz shown in Figures 3(a), (b), (c). The above figure clearly shows the excitation of CSRRs at 4.96 GHz.

### 3. Q FACTOR AND COUPLING COEFFICIENT CALCULATION

The crucial parameters that can be found based on the circuit components of an lowpass filter (LPF) are the quality factor and coupling coefficients. The proposed filters offset distances  $e_1$  and  $e_2$  are obtained with the correlation between  $Q$  factor and coupling coefficient. The offset distance would be adjusted in CST to attain their correlation with the  $Q$  factor and coupling coefficient. The unloaded quality factor and coupling coefficient vs offset distance responses are illustrated in Figure 4(a). The simulated unloaded  $Q$  factor and coupling coefficient for the proposed filter is 508 and 0.011. The proposed filter group delay is 9 ns and 1.5 ns maximum difference within the passband shown in Figure 4(b).

The loaded  $Q$  factor of a cavity is defined by

$$Q_l = \frac{f_0}{\Delta f} \tag{2}$$

where  $f_0$  is the midband resonant frequency, and  $\Delta f$  is  $-3$  dB bandwidth.

The external  $Q$  factor is given by

$$Q_e = \frac{Q_l}{10^{\frac{-IL}{20}}} \tag{3}$$

where  $IL$  is the insertion loss of  $S_{21}$  at midband frequency.

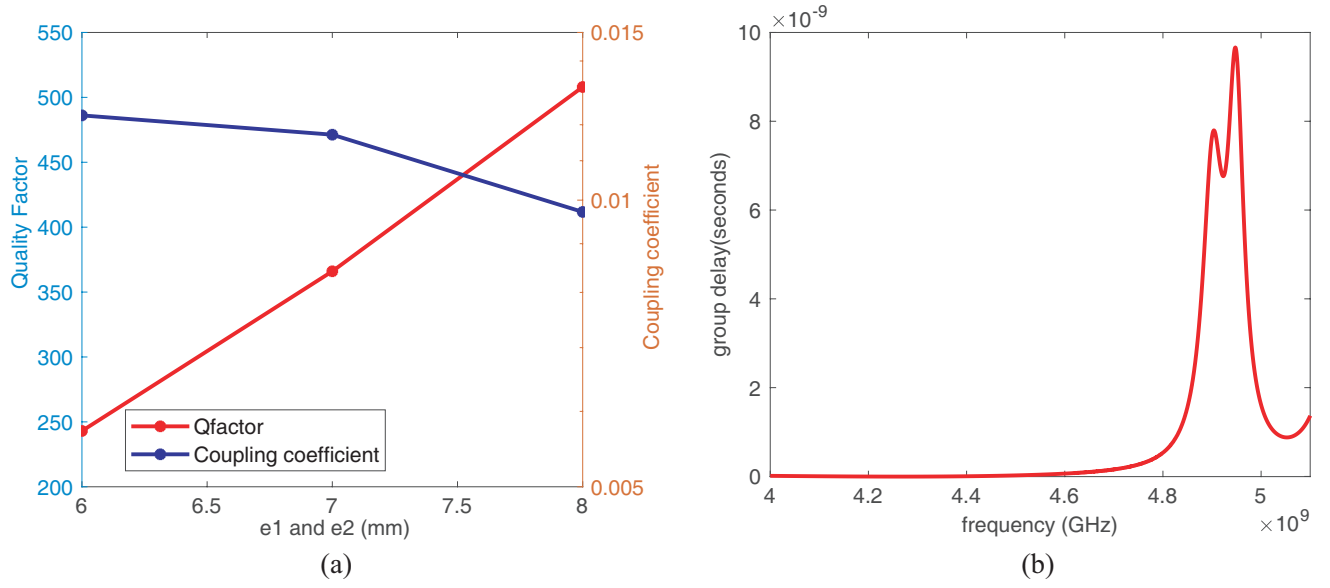


**Figure 4.** (a) Coupling coefficient, quality factor vs  $e_1$  and  $e_2$  (mm). (b) Group delay.

The unloaded  $Q$  factor is given by

$$\frac{1}{Q_u} = \frac{1}{Q_l} - \frac{1}{Q_e} \quad (4)$$

The coupling coefficient is given by

$$k = \frac{f_2^2 - f_1^2}{f_2^2 + f_1^2} \quad (5)$$

$f_1$  is the low mode frequency, and  $f_2$  is the high mode frequency

#### 4. PARAMETRIC ANALYSIS

The proposed SIW filter performance is analyzed using parametric assessment. The perturbing metallic via centre-to-centre spacing varies from  $p_1 = 1.2$  to 1.6 mm. Its corresponding  $S$  parameter results are depicted in Figure 6(a), which shows that the coupling does not occur at 1.4 mm and 1.6 mm. Figure 6(b) illustrates the filter response changes corresponding to the offset length changes of  $e_1$  and  $e_2$ . When  $e_1$  and  $e_2 = 8$  mm, the CSRR couples the cavity's first and second modes, resulting in a two-pole narrowband filter with two transmission zeros. It does not occur for the other two values (6 mm, 7 mm). Likewise, the varied positions ( $p = 1, p = 2, p = 3, p = 4$ ) of CSRRs are depicted in Figures 5(a)–(d), and corresponding  $S$  parameters are shown in Figure 6(c). When  $R_1$  and  $R_2$  resonators slit gaps are oriented towards the top or bottom, the desired filter response is obtained. When  $R_1$  and  $R_2$  resonators slit gaps are at the positions  $p = 3$  and  $p = 4$ , the filter exhibits an under-coupled passband and higher insertion loss. Next,  $R_1$  and  $R_2$  resonators slit gaps are rotated  $180^\circ$  away from the perturbing via,

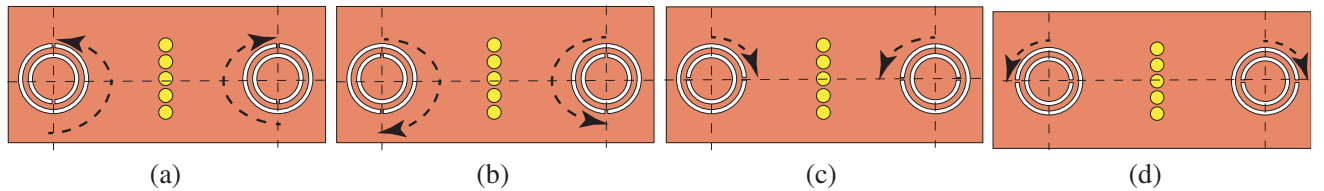


**Figure 5.** Open gap of the CSRR's facing. (a) Top. (b) Bottom. (c) Side front to front. (d) Side back to back.

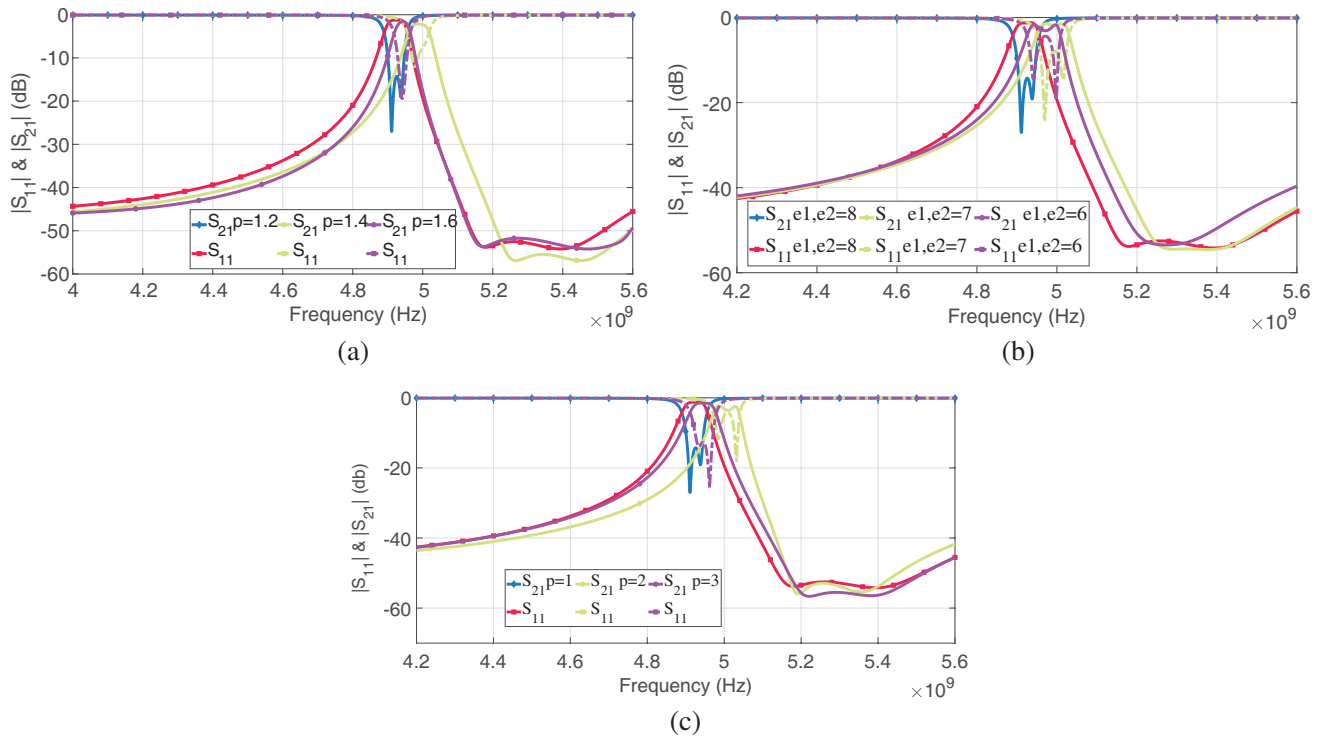


**Figure 6.** *S* parameter variations. (a) Varying  $p_1$  (mm). (b) Varying  $((e_1$  and  $e_2$  (mm)). (c) Varying positions of the CSRR.

failing to produced passband. When  $R_1$  slit gap is towards the perturbing via, and  $R_2$  slit gap is rotated  $180^\circ$  away from the perturbing via or vice versa, the passband does not occurs. Hence, this shows the existence of mixed coupling between the CSRR and perturbing via. The optimum values obtained for the proposed filter are  $p_1 = 1.2$  mm,  $e_1, e_2 = 8$  mm, and slit gaps are facing towards the top.

### 5. RESULTS AND DISCUSSIONS

The fabricated narrowband filter shown in Figure 1 uses one layer RTduroid 5880 with thickness of the dielectric = 0.51 mm, dielectric constant  $\epsilon_r = 2.2$ , and  $\tan \delta = 0.0009$ . Its top and bottom views are illustrated in Figure 7(a) and Figure 7(b). The response of the filter is measured by Anritsu vector network analyzer MS-46122B. The fabricated response slightly differs from the simulated one due to fabrication tolerances and soldering of SMA connectors. It is illustrated in Figures 7(c) and (d). The measured insertion loss of the filter is 2.9 dB with a fractional bandwidth of 1.16%. The filter’s centre frequency is 4.947 GHz with an unloaded  $Q$  factor of 302.

The comparison table compares the narrowband filter of microstrip [14,17] and SIW technology [9,15,16,18]. From Table 1, it can be inferred that the proposed narrowband filter is simple in structure with one layer and one cavity. But the existing works [15,18] used 3, 4 layers, and [9,16] used 3, 2 cavities in designing a narrowband filter. The fractional bandwidth is less than 1%, and the center frequency is less than 1 GHz for the microstrip filter reported in [14]. The insertion loss of the proposed filter is 2.11 times [16] and (1.8–2.53) times [17] less than the existing works. The size of the proposed filter is 25% [16] and 117% [9] less than the existing SIW counterparts. Hence, the proposed filter with a simple structure, high selectivity, compact size, and low insertion loss is designed for sub-6 GHz applications.

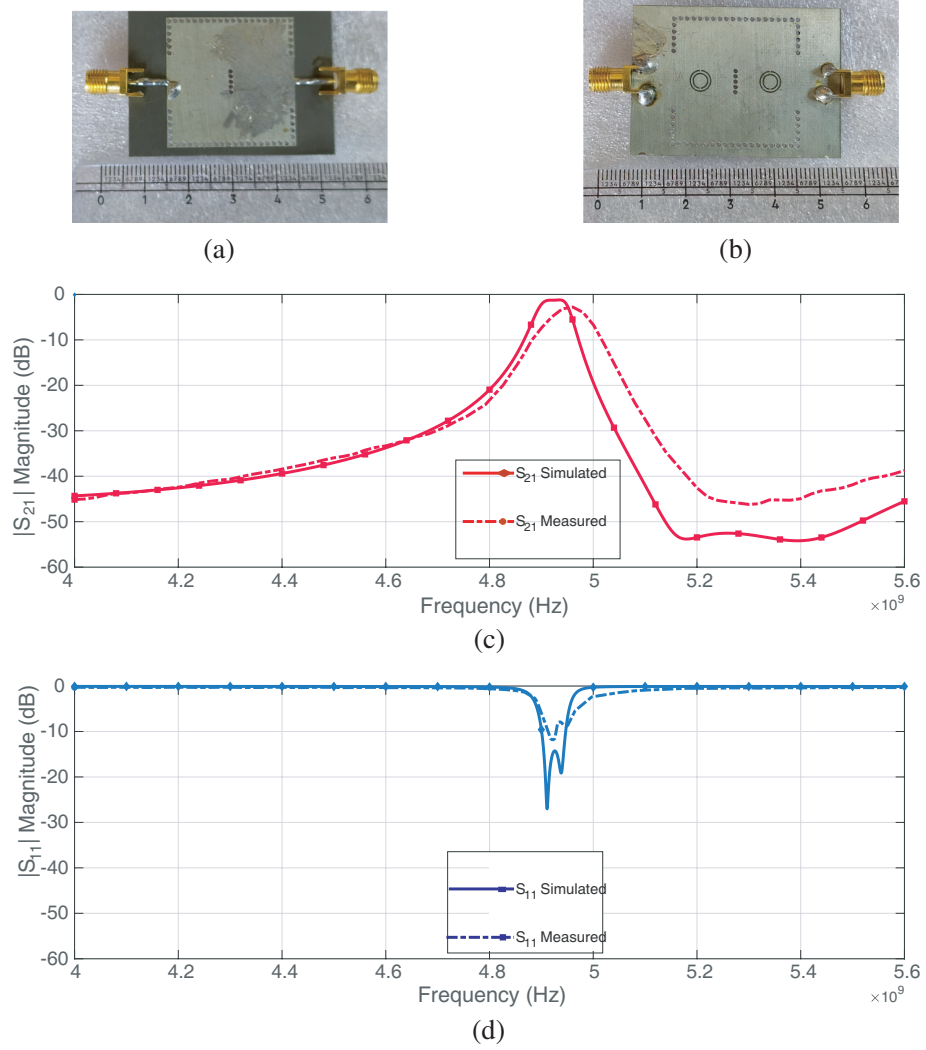


**Figure 7.** Fabricated prototype. (a) Front view. (b) Back view. (c) Comparison of simulated and measured results  $|S_{21}|$  dB. (d)  $|S_{11}|$  dB for  $p = 1$  ( $R_1$  and  $R_2$ ) resonators slit gaps are oriented towards the top.

**Table 1.** Comparison of present literature report.

Ref.	$f$ (GHz)	$FB$ (%)	$IL$ (dB)	No. of Layers	No. of Cavity
9	8.25	1.1	3.3	1	3
14	0.845	0.17	0.55	1	/
15	11	3	2.15	3	/
16	5.8	2.51	6.35	1	2
17	(0.022–0.004)	2.4	(5.4–7.6)	1	/
18	34.5	2.5	1.7	4	1
This work	4.947	1.16	2.9	1	1

FB is fractional bandwidth, IL is insertion loss

## 6. CONCLUSION

A high selectivity narrowband bandpass filter (BPF) with two transmission zeros on the upper stopband is designed with SIW technology. The SIW cavity with perturbing vias is loaded with two CSRRs on either side of the perturbing vias which constitute a narrowband filter. The coexistence of electric and magnetic coupling due to perturbing elements and the CSRR provides mixed-coupling in the proposed structure. The CSRRs are involved in creating two transmission zeros on the upper out of band with a reduction in size. The proposed filter is a second-order BPF with good roll-off and higher unloaded quality factor  $Q$  used for sub-6 GHz applications. The proposed filter has sharper selectivity and less than 2% fractional bandwidth. The filter with these characteristics can be used in diplexer and oscillator. The merits of the proposed filter are simple, single cavity, single layer, and utilizes full mode SIW. The work can be extended with box topology in a single cavity embedded with CSRRs to have multiband characteristics.

## REFERENCES

1. Huang, J., G. Dong, J. Cai, H. Li, and G. Liu, "A quad-port dual-band MIMO antenna array for 5G smartphone applications," *Electronics*, Vol. 10, No. 5, 542–547, 2021.
2. Deslandes, D. and K. Wu, "Single-substrate integration technique of planar circuits and waveguide filters," *IEEE Transactions on Microwave Theory and Techniques*, Vol. 51, No. 10, 593–596, 2003.
3. Matthaei, G. L., E. M. T. Jones, and L. Young, *Microwave Filters, Impedance-matching Networks, and Coupling Structures*, 217–228, Artech House, Norwood, MA, 1980.
4. Kumar, A., D. Chaturvedi, and S. I. Rosaline, "Design of antenna-multiplexer for seamless on-body Internet of Medical Things (IoMT) connectivity," *IEEE Transactions on Circuits and Systems II: Express Briefs*, Vol. 69, No. 8, 3395–3399, Aug. 2022.
5. Praveena, N. and N. Gunavathi, "Realization of dual-mode, high-selectivity SIW cavity bandpass filter by perturbing circular shape vias," *Appl. Phys. A*, Vol. 128, No. 773, 2022.
6. Soundarya, G. and N. Gunavathi, "Compact dualband SIW bandpass filter using CSRR and DGS structure resonators," *Progress In Electromagnetics Research Letters*, Vol. 101, 79–87, 2021.
7. Zhu, F., G. Q. Luo, B. You, X. H. Zhang, and K. Wu, "Planar dual-mode bandpass filters using perturbed substrate-integrated waveguide rectangular cavities," *IEEE Transactions on Microwave Theory and Techniques*, Vol. 69, No. 6, 3048–3057, 2021.
8. Zhang, H., W. Kang, and W. Wu, "Miniaturized dual-band SIW filters using E-shaped slotlines with controllable center frequencies," *IEEE Microw. Wireless Compon. Letters*, Vol. 28, No. 4, 311–313, 2018.
9. Khan, A. A. and M. K. Mandal, "Narrowband substrate integrated waveguide bandpass filter with high selectivity," *IEEE Microwave and Wireless Components Letters*, Vol. 28, No. 5, 416–418, 2018.
10. Liu, Q., D. Zhang, M. Tang, H. Deng, and D. Zhou, "A class of box-like bandpass filters with wide stopband based on new dual-mode rectangular siw cavities," *IEEE Transactions on Microwave Theory and Techniques*, Vol. 69, No. 1, 101–110, 2021.
11. Liu, Z., G. Xiao, and L. Zhu, "Triple-mode bandpass filters on CSRR loaded substrate integrated waveguide cavities," *IEEE Trans. Compon., Packag., Manuf. Technol.*, Vol. 6, 1099–1105, 2016.
12. Geng, Q. F., H. J. Guo, Y. Y. Zhu, et al., "A novel dual-band filter based on single-cavity CTSRR-loaded triangular substrate-integrated waveguide," *International Journal of Microwave and Wireless Technologies*, Vol. 11, 894–898, 2019.
13. Wu, L. S., X. L. Zhou, Q. F. Wei, et al., "An extended doublet Substrate Integrated Waveguide (SIW) bandpass filter with a Complementary Split Ring Resonator (CSRR)," *IEEE Microwave and Wireless Components Letters*, Vol. 19, 777–779, 2009.
14. Huang, X., X. Guan, B. Ren, and S. Wan, "A novel HTS ultra-narrowband bandpass filter using hairpin meander-line resonator with gradient line-width," *IEEE Transactions on Applied Superconductivity*, 2022.

15. Máximo-Gutiérrez, C., J. Hinojosa, and A. Álvarez-melcon, “Narrowband and wideband bandpass filters based on empty substrate integrated waveguide loaded with dielectric elements,” *IEEE Access*, Vol. 9, 32094–32105, 2021.
16. You, C. J., Z. N. Chen, X. W. Zhu, and K. Gong, “Single-layered SIW post-loaded electric coupling-enhanced structure and its filter applications,” *IEEE Transactions on Microwave Theory and Techniques*, Vol. 61, No. 1, 125–130, 2013.
17. Zakharov, A., S. Rozenko, S. Litvintsev, and M. Ilchenko, “Hairpin resonators in varactor-tuned microstrip bandpass filters,” *IEEE Transactions on Circuits and Systems II: Express Briefs*, Vol. 67, No. 10, 1874–1878, 2020.
18. Shen, M., Z. Shao, X. Du, Z. He, and X. Li, “Ka-band multilayered substrate integrated waveguide narrowband filter for system-in-package applications,” *Microwave and Optical Technology Letters*, Vol. 58, No. 6, 1395–1398, 2016.